Lasers in Medical Science (2024) 39:24
https://doi.org/10.1007/s10103-023-03955-3

ORIGINAL ARTICLE

# In vivo attenuation profile of 660 nm and 830 nm wavelengths on human elbow skin and calcaneus tendon of different phototypes

**Carlos Eduardo Girasol[1] · José Miguel Andrade Ferraz Moraes[2] · Luciano Bachmann[3] · Damião Miranda Ngonga Alfredo[1,4] · Rafael Inácio Barbosa[5] · Elaine Caldeira de Oliveira Guirro[1] · Rinaldo Roberto de Jesus Guirro[1]**

Received: 10 June 2021 / Accepted: 11 December 2023


## Abstract

Physical factors and tissue characteristics determine the transmission of light through tissues. One of the significant clinical limitations of photobiomodulation is the quantification of fluence delivered at application sites and optical penetration depth in vivo. There is also the difficulty of determining the distances of the application points to cover a uniformly irradiated area. Thus, the aim was to evaluate in vivo the influence of melanin on light transmission of the 660 nm and 830 nm laser wavelengths on skin and tendon. Thirty young individuals of both sexes were recruited, divided into two groups based on melanin index, and submitted to photobiomodulation protocols in the posterior region of the elbow (skin-skin) and the calcaneus tendon (skin-tendon-skin). The irradiation area was evaluated using a homemade linear array of five sensors. We found significant transmission power values for different melanin indexes and wavelengths ($p<0.0001$). Also, different equipment can generate significant differences in the transmitted power at an 830-nm wavelength. Average scattering values are 14 mm and 21 mm for 660 nm, in higher and lower melanin index, respectively. For 830 nm, values of 20 mm and 26 mm are indicated. Laser light transmission in vivo tissues is related to wavelength, beam diameter, tissue thickness, and composition, as well as melanin index. The 830-nm laser presents higher light transmission on the skin than 660 nm. The distances between the application points can be different, with higher values for 830 nm than 660 nm.

**Keywords** Physical therapy · Power · Penetration · Tendon · Skin · Photobiomodulation

## Introduction

Photobiomodulation has grown significantly in the last decade, ratifying the mechanisms of action established in the literature and expanding the stimulated responses of photon interactions with cells and organelles. The term is related to the application of low-power light (<500 mW) to biological tissues, applying therapy with a non-ionizing, non-thermal light source, independent of the laser probe and located between visible or near-infrared wavelengths, promoting photophysical and photochemical phenomena at different biological scales [1–3]. The cellular alterations stimulated by the absorption of light by the cytochrome c-oxidase (CCO) or IV complex, besides the interaction in the mitochondrial electron transport chain [4], refer to positive clinical repercussions, such as fatigue reduction [5], increased performance [6], skin healing [7, 8], analgesia [9], and neuroprotective effects in a series of disorders affecting the central nervous system [10]. The CCO is a terminal

✉ Rinaldo Roberto de Jesus Guirro
rguirro@fmrp.usp.br

1 Postgraduate Program in Rehabilitation and Functional Performance, Department of Health Sciences, Ribeirão Preto Medical School of the University of São Paulo (USP), Ribeirão Preto, São Paulo, Brazil

2 Graduation in Physical Therapy, Ribeirão Preto Medical School of the University of São Paulo (USP), Ribeirão Preto, Brazil

3 Postgraduate Program in Physics Applied to Medicine and Biology, University of São Paulo (USP), Ribeirão Preto, Brazil

4 School of Health Sciences and Sports, Methodist University of Angola (UMA), Luanda, Angola

5 Postgraduate Program in Rehabilitation Sciences, Federal University of Santa Catarina (UFSC), Araranguá, Brazil

Published online: 09 January 2024

enzyme of the respiratory chain in eukaryotic cells mediating the transfer of electrons from cytochrome c to molecular oxygen [4]. This chemical reaction interferes directly with the cell production energy. Thus, CCO is also considered the photoacceptor and photosignal transducer in the visible and near-infrared region [4, 11]. To obtain efficient therapeutic results, it is essential to adequately select photonic parameters, thus avoiding adverse or ineffective effects [12]. In this context, there is an added difficulty in adjusting the fluence that should reach the target tissue, considering the reflection, refraction, scattering, and absorption of light by tissues [13].

In this way, studies that address the light-tissue interaction and optimize the photobiomodulation outcomes are highlighted. For example, the color and thickness of the skin affect the transmittance and scattering of the laser and should be considered in the selection of the energy density (fluence) to ensure therapeutic efficacy [13]. Ash et al. [14] simulated light penetration into the skin, varying beam width and wavelength, and reported that the highest values of beam area (40 mm) and wavelength (750 nm) are related, in order, to the lowest dispersion and the highest depth. In the same line, Barbosa et al. [15] analyzed the laser transmissivity in the wavelengths of 660, 830, and 904 nm in rat skin and pigskin, fat, and muscle. In addition to reporting results of transmissivity, the authors discuss the need to know the properties of the laser beam and the optical properties of biological tissues in vivo to make treatments more effective.

A point that is still little discussed in the literature of photobiomodulation is the attenuation and scattering that light suffers when penetrating the tissues. Considering that absorption, scattering, and refraction of light reduce the fluence deposited that reaches the target structures at the skin's subsurface, it is important to study the light-tissue interaction to know the fluence at the depths in which the target chromophores are found. Some of the therapeutic targets may be several centimeters deep, such as muscles, tendons, peripheral nerve, and cartilage [16–18], a fact that favors the loss of power that reaches the target cell and, consequently, the loss of efficiency of the intervention. Nussbaum, Zuylen, and Jing [19] point out that among the scattering elements in superficial skin tissue, one can include cell membranes, melanin, hemoglobin, collagen fibers, interfaces between layers with different refractive indexes, and blood vessels. Light absorption in the tissue, on the other hand, is mainly caused by hemoglobin in the dermis, subcutaneous lipids, and melanin in the skin, which depends on individual conditions [19–21].

There is extensive literature that can be found on the optical properties of skin that have been obtained in vitro and in vivo [20, 22–24]. However, there is a clear need to know the optical properties in vivo or light penetration that effectively reach the target cells under the skin, such as in muscle or tendon, for example.

Moreover, clinically, one of the significant limitations is the empirical determination of the spacing between application sites. The light diffusion on different tissues is not well known [25]. Thus, this study aimed to evaluate the in vivo influence of the melanin index on the attenuation of laser wavelengths (660 nm and 830 nm) in skin and tendon and better infer the separation sites of therapeutic applications to produce a more homogeneous light delivery.

## Material and methods

### Ethics

This study was approved by the Ethics Committee of the Clinics Hospital of the Medical School of Ribeirão Preto under protocol 2.748.430. The research was carried out at the Laboratory of Physiotherapeutic Resources (LARF) of the Medical School of Ribeirão Preto of the University of São Paulo (FMRP-USP). The volunteers were informed about the research project, its objectives, and its characteristics, and all signed the consent form.

### Participants

A total of 30 individuals, aged between 18 and 40 years, of both sexes, with no history of systemic skin lesions located on the elbow or ankle-foot, were recruited.

Melanin index and tissue thickness were measured on the posterior face of the elbow ("skin-skin") and in the lateral face on the calcaneus tendon ("skin-tendon-skin"). Both data acquisitions were conducted bilaterally on the 30 individuals, with three sequential evaluations performed by an experienced examiner, considering the mean value of each segment.

To measure the melanin index, the Cutometer MPA 580 (Courage + Khazaka Electronic, Köln, Germany) was used to probe the Mexameter calibrated according to the manufacturer's guidelines. The tests were performed in a controlled setting, with room temperature at 22 ± 3 °C and relative humidity of 60%. The participants were seated, with their limbs at rest, and were acclimatized for 10 min before starting the tests. The probe was then touched to the areas of evaluation interest, and for the upper limb, the individual maintained a seated position with the elbow extended (evaluation of the lateral aspect of the elbow skin) and for the lower limb, the individual was lying down with the ankle in neutral (evaluation of the lateral aspect of the calcaneal tendon).

The thickness in "skin-skin" and "skin-tendon-skin" conditions was quantified on both limbs with an electronic micrometer (DIGIMESS, São Paulo, SP, Brazil).

After the initial evaluation, the volunteers were divided into two groups, from the melanin index: "light skin" group, constituted by individuals that presented values lower than 500 (half of the equipment scale) and "dark skin" for those above 500. As a description, indices higher than 500 would be related to a scale higher than V on the Fitzpatrick Scale [26]. Such values were derived from the scale with variation from 0 to 1000 of the equipment itself.

## Photobiomodulation

Two different types of photobiomodulation equipment were used, and their parameters are presented in Table 1. The power, beam diameter, and divergence of each were checked before use. The manufacturers were contacted to provide more details about the diode specifications, such as laser beam operation, beam size, and power density at the probe.

The applications were performed in a controlled environment, with ambient temperature at 22 ± 3 °C and relative humidity of 60%, at the wavelengths of 660 and 830 nm, in the pulsed regime for both types of equipment, in all conditions ("skin-skin" and "skin-tendon-skin") and wavelengths (660 nm and 830 nm).

The beam diameters were collected using a visible radiation-sensitive detector (LM-2 Vis, Coherent, USA) for the 660-nm laser and a near-infrared radiation-sensitive detector (LM-2 NIR, Coherent, USA) for the 830-nm laser. A power meter (FieldMaxII TOP, Coherent, USA) was used for both detectors. The detectors were equipped with an SMA optical adapter (SubMiniature A connector—Type, Coherent, USA), to which a 10 cm segment of fiber optics with a diameter of 0.4 mm was attached. Two micrometric displacement devices with 0.005-mm resolution were used to move the detector along the longitudinal and transversal axis of the laser beam. The fiber optic tip was initially positioned longitudinally ($z = 0$) and moved transversally, covering the entire beam irradiation field. With this measurement, it was possible to determine the transversal profile of the beam to $z = 0$, the contact position, and calculate the beam diameter. For each measurement, the beam diameter was determined using a Gaussian function. To assess the beam profile for the various pieces of equipment, the average power across the entire beam cross-section was measured. This procedure was repeated for the $z = 3$-, 4-, 12-, and 15-mm positions so that it was possible to measure the same profile for different distances from the light source. The entire procedure was performed for both lasers and wavelengths (Table 2).

**Table 1** Technical characteristics of the employed equipment

| | Equipment 1* | | Equipment 2# | |
|---|---|---|---|---|
| Information provided by manufacturers | | | | |
| Laser operation | Continuous | | | |
| Laser delivered | Pulsed | | | |
| Pulse repetition rate (Hz) | 150 | | 100 | |
| Wavelength (nm) | 660 | 830 | 660 | 830 |
| Laser probe area ($cm^2$) | 0.06 | 0.12 | 0.10 | 0.10 |
| Power density ($W/cm^2$) | 0.28 | 0.13 | 0.13 | 0.15 |

*Laserpulse (Ibramed, Amparo, São Paulo, Brazil)

#Photon Lase III (DMC, São Carlos, São Paulo, Brazil)

## "Skin-skin" and "skin-tendon-skin" transmission

We assembled five silicon photodiode sensors (SFH 206K, Farnell, USA) coupled side by side, with a 35-mm-long linear array of detectors to capture the light transmitted by the irradiated tissues. They had their optimum sensitivity for the red and infrared spectrum, with their peak (100%) occurring at 900 nm. For the 830-nm and 660-nm spectra, they had 95% and 65% sensitivity, respectively. The sensors were connected to amplifiers and these to an electronic prototyping board (UNO R3, Arduino, Italy) and an analog-digital converter (ADS 1115, Texas Instruments, Dallas, TX, USA). This system allowed data acquisition in a VivoBook notebook (Asus, Cajamar, São Paulo, Brazil) using the platform PLX-DAQ version 2. The data was arranged in columns in the Excel software (Microsoft Corporation by Impressa Systems, Santa Rosa, CA, USA) for

**Table 2** Determination of the beam diameter of the equipment used

| Wavelength | Equipment 1 | | Equipment 2 | |
|---|---|---|---|---|
| | 660 nm | 830 nm | 660 nm | 830 nm |
| Average power | 17 | 15 | 13 | 15 |
| Distance from the emitter | Beam diameter—mm (SD) | | | |
| 0 mm | 0.41 (0.00) | 0.32 (0.00) | 0.53 (0.02) | 0.72 (0.02) |
| 3 mm | 0.77 (0.03) | 0.66 (0.01) | 1.23 (0.06) | 1.72 (0.13) |
| 4 mm | 0.98 (0.04) | 0.85 (0.02) | 1.48 (0.08) | 2.21 (0.27) |
| 12 mm | 1.93 (0.08) | 1.85 (0.02) | 1.57 (0.14) | 4.03 (0.83) |
| 15 mm | 2.53 (0.08) | 1.74 (0.04) | 2.07 (0.26) | 4.80 (1.09) |

*SD* Standard deviation

real-time measurement. The system was gauged with the same FieldMaster equipment used in this study and previously described: with a near-infrared and visible sensor. It is important to notice here that this measurement acquired the light transmission at five single points to measure the transmitted light in vivo at "skin-skin" and "skin-tendon-skin" samples.

To assess transmitted power in the "skin-skin" condition, volunteers were seated with the upper limb resting on an examination table. A scientific adipometer pulled the skin of the posterior region of the elbow (Sanny, model AD1011-LD) fixed to the photodiode array. The laser probe was set to a rigid support, which allowed the perpendicular application in contact with the skin on the opposite face to the one in touch with the photodiode array (Fig. 1B).

In the "skin-tendon-skin" condition, the volunteers were in a comfortable seated position with a neutral ankle position. The photodiode array was placed on the lateral side of the calcaneus tendon, with the laser probe attached to the medial side, perpendicular to the tendon, and the photodiode sensors attached to the adipometer (Fig. 1C).

For both conditions ("skin-skin" or "skin-tendon-skin"), the data collections were repeated for both limbs. We also notice that the holder for the laser probe and adipometer was important to standardize the position of laser application and pressure for thickness measurement.

## Data processing and statistical analysis

To estimate the light attenuation in vivo, the attenuation coefficient ($\mu_a$) was calculated considering Beer-Lambert's law [27]. In this way, we considered the equation 1:

$$I = (1 - R)I_0 e^{-\mu_a t} \quad (1)$$

where $R$ is the skin reflectance, $\mu_a$ is the attenuation coefficient, $t$ the thickness of the skin, $I_0$ the incident power, and $I$ the transmitted power. For the skin reflectance, we considered the values from Mendenhall et al., with a range of skin reflectance values between ≅ 0.1 and 0.5 [28].

In this manner, from Beer-Lambert's law, the average attenuation coefficient was calculated. For the "skin-skin" condition, the double skin layer was considered. For the "skin-tendon-skin" condition, the double skin layer plus the tendon was considered. According to the mentioned methodology, we calculated the light power after the first layer of tissue, considering the power at half thickness, i.e., considering the attenuation of the light going through the double layer of skin.

For statistical analysis, the Kolmogorov–Smirnov normality test was used to verify the data distribution [29]. The Kruskal–Wallis test with Dunn's multiple comparisons was used to evaluate the differences between the power emitted and the power transmitted after irradiation in tissues [30]. The Mann–Whitney test was applied to assess the transmission between the melanin index and emission sources. When parametric, a paired $t$ test was used.

For the correlation between transmission and thickness, the Spearman correlation test ($r_s$) was used [31], considering all 30 volunteers (60 samples) for the analysis. Finally, to evaluate the proportion of the variance between these variables, a linear regression was performed, where the description of the proximity between the data was presented by means of the $R$-squared ($r^2$). For all tests, the $p$ value of $< 0.05$ was considered to represent the value used for the research issue and considering the sample size. It

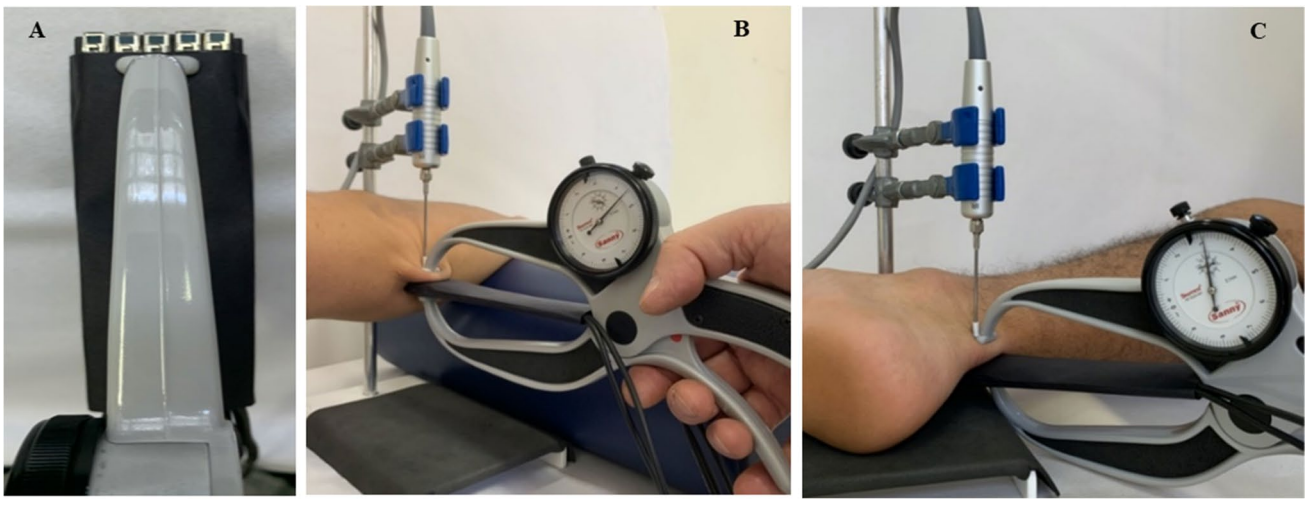


**Fig. 1** Instrumentation and data acquisition procedures. **A** Photodiode sensors coupled to adipometer clamp, **B** "skin-skin" data acquisition at the elbow with the laser prove upside, adipometer clamp and between the photodiode array; **C** The same as described before in part (B) but applied for the "skin-tendon-skin" data acquisition

thus corresponds to a confidence level of 95% for decision support. Data processing was performed in GraphPad Prism software version 7.0 (GraphPad Software, San Diego, CA, USA).

## Results

A total of 30 volunteers were recruited, with an average age of 24.5 years (SD = 4.9). The volunteers were divided into two groups after the evaluations, being distinct between "light skin" ($n = 15$) and "dark skin" ($n = 15$), according to the value found in the melanin index evaluation. The characterization values can be found in Table 3, presented in mean and SD.

The volunteers were evaluated, bilaterally, in 60 samples, both for "skin-skin" analysis in the upper limb and for "skin-tendon-skin" in the lower limb.

In Table 4, we observe the average values for the incident power, calculated at half-thickness ($I_{t/2}$) and measured at full thickness $t$ ($I_t$) for samples with a higher index of melanin (>500) and lower index of melanin (<500). It is important to notice that the incident power and the power at full thickness were measured while the value at half-thickness was calculated, according to Beer-Lambert's law. The transmitted power is presented in absolute values (mW) and also in percentage transmission (%). This table presents values for both employed equipment. Figure 2 exemplifies the

**Table 3** Characterization of the sample in both groups

| Variables | Light skin | Dark skin |
|---|---|---|
| Age (years) | 22.47 (3.02) | 26.60 (5.64)* |
| Weight (kg) | 65.89 (9.78) | 73.36 (14.17) |
| Height (m) | 1.69 (0.07) | 1.77 (0.07)* |
| Body mass index (Kg/m$^2$) | 21.62 (6.49) | 23.3 (3.13) |
| Thickness of skin-skin (mm) | 3.02 (0.16) | 3.86 (0.11)* |
| Melanin index at skin-skin | 326.70 (79.06) | 855.88 (185.1)* |
| Thickness of skin-tendon-skin (mm) | 12.60 (0.46) | 15.15 (0.55)* |
| Melanin index of skin-tendon-skin | 269.36 (82.21) | 746.56 (179.1)* |

*$p < 0.05$

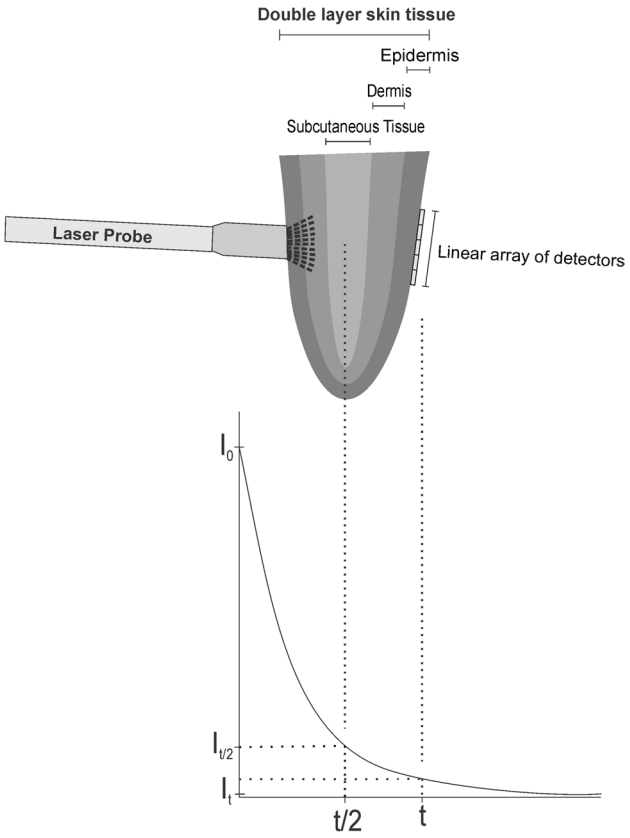


**Fig. 2** Laser probe positioning, measured ($I_t$) and calculated ($I_{t/2}$) power

**Table 4** Average incident power ($I_0$) and average power at half-thickness value ($I_{t/2}$) and at total-thickness value ($I_t$) of the irradiated tissue. The attenuation values for the power can be visualized in absolute values (mW) and percentage values (%)

| | | Skin-skin | | | | | | | | Skin-tendon-skin | | | | | | | |
|---|---|---|---|---|---|---|---|---|---|---|---|---|---|---|---|---|---|
| | | >500 | | | | <500 | | | | >500 | | | | <500 | | | |
| | $I_0$ (mW) | $I_{t/2}$ | | $I_t$ | | $I_{t/2}$ | | $I_t$ | | $I_{t/2}$ | | $I_t$ | | $I_{t/2}$ | | $I_t$ | |
| | | mW | % | mW | % | mW | % | mW | % | mW | % | mW | % | mW | % | mW | % |
| IR-E1 | 15 | 1.14 | 7.6 | 0.04 | 0.3 | 1.41 | 9.4 | 0.07* | 0.5 | 0.46 | 3.0 | 0.00 | 0.0 | 0.36 | 2.4 | 0.01* | 0.0 |
| R-E1 | 17 | 1.08 | 6.4 | 0.04 | 0.2 | 1.99 | 11.7 | 0.14* | 0.8 | 0.55 | 3.2 | 0.01 | 0.1 | 0.58 | 3.4 | 0.01* | 0.1 |
| IR-E2 | 15 | 2.02 | 13.5 | 0.14$^{\#}$ | 0.9 | 2.23 | 14.9 | 0.17*$^{\#}$ | 1.1 | 0.73 | 4.9 | 0.02$^{\#}$ | 0.1 | 0.94 | 6.3 | 0.03*$^{\#}$ | 0.2 |
| R-E2 | 13 | 1.04 | 8.0 | 0.04 | 0.3 | 1.99 | 15.3 | 0.14* | 1.0 | 0.32 | 2.5 | 0.00 | 0.0 | 0.49 | 3.7 | 0.01*$^{\#}$ | 0.1 |

*IR* Near-infrared; *R* red; *E1* equipment 1; *E2* equipment 2; *mW* miliwatts; <500 and >500: melanin index; $I_{t/2}$ half-thickness value; $I_t$ total-thickness value; *difference between $I_t$ (<500) versus respective >500 ($p < 0.05$); $^{\#}$difference between $I_t$ (<500) versus the same wavelength and melanin index in a different equipment

calculation sites and measurement of the respective transmitted powers, as shown in the table.

A lower value for transmitted power was observed for the samples with a higher melanin index, with more significant differences for the red wavelength. For skin-tendon-skin irradiation, transmission is considerably lower, which is practically zero for samples with a higher melanin index.

Compared to the same wavelength in the different equipment, the near-infrared spectrum showed a significant difference ($p < 0.0001$) for the mean power transmitted regardless of the melanin index or region of application. For the red spectrum, no significant difference was observed regardless of the observed variables.

To measure the influence of melanin, thickness, and wavelength on the light transmission, a linear correlation was evaluated (Fig. 3). The analysis was conducted only for the elbow measurement skin-skin given the skin-tendon-skin measurement showed a transmitted power close to zero. Correlations for the red wavelength were higher for the melanin index ($r_s = -0.786$) and moderate for thickness ($r_s = -0.512$). In the near-infrared spectrum, they were weaker for both.

The spread light after transmission by skin-skin and skin-tendon-skin irradiation was evaluated at five sites (Fig. 4). The photodiode in the middle measures the central value for the transmitted power, and the other four lateral photodiodes measure the spread light after transmission. In all sample sets, we observe a peak value at the central point (CP) position.

For the "skin-skin" collections, a distribution with the presence of a central peak and uniform decay was observed bilaterally for the different melanin index and wavelengths, with higher average power values for 830 nm. For the "skin-tendon-skin" collections, this pattern was not observed. Although the transmitted power was observed, the values were not sufficient to draw a profile described for the skin–skin condition. Apparently, although transmission occurs, it is due strongly to lateral scattering and with a large presence of light absorption factors up to this point of analysis. It is emphasized that the image of the distribution is on the scale of the sensors, making 35 mm of full extension, fractioned at each 7 mm (Fig. 4).

To provide homogeneous irradiation, it is important to provide a separation of irradiation sites over the desired skin area that delivered the same light distribution (fluence) after the skin. Thus, Fig. 5 shows what should be considered since the distance between the points is a predetermining factor for a uniform application and with responses to all the cells reached.

For calculating the distance between two application sites, the incident power of 50% in the lateral sensors to the central sensor was considered, along with the equipment, wavelengths, and melanin index. For that, a linear regression was applied, and the observed value of the intercept and slope was considered for the following Eq. (2):

$$I = a + b * x \tag{2}$$

where $I$ is the intensity, $a$ is the intercept, $b$ is the slope, and $x$ is the distance to be found, where for the study, it was considered 50% of the straight line. This way, the point where the intensity represents 50% of the maximum intensity is observed, making it possible to calculate the overlapping value of the points to point out a possible distance between the applications.

The value presented in Table 5 is equivalent to twice the distance collected in the sensors, indicating that equipment 2 (E2) showed the shortest and longest distance for the red and near-infrared spectra, respectively, associated with a higher and lower melanin index.

## Discussion

The interest in the transmission of light in human tissues is an old question [32]. However, currently, there is still a gap in the literature due to the lack of methodological quality and reliable conclusions. The indications of the distances between the points of application are given empirically since there is no literature to support them, and sometimes clinical studies use them. Thus, references about the scattering in biological tissues and its clinical outcome, to our knowledge, are not yet available to the scientific community and clinical practice. Therefore, our study offers innovative data regarding the distance between the points of application and the scattering in different melanin indices in human tissue. In turn, data, such as transmissivity, are more present, but still with methodological limitations pointed out by the literature. Studies with different wavelengths and tissues were explored [33–35] and other therapeutic resources. Thus, Guirro et al. [36] analyzed the transmissivity of photobiomodulation (660, 830, and 904 nm) in thirteen occlusive dressings used for the treatment of skin lesions and concluded that transmission depends on the material of the occlusive dressing, its thickness, and wavelength.

Among the therapeutic options, besides the point of light-emitting sources, you can have sources, such as blankets and clusters. Guirro et al. [37] proposed using a blanket for irradiation to cover a larger area and consequently decrease the total time of therapy. For example, such techniques favor application next to thighs and calves, among other extensive muscle groups. In turn, the use of the cluster is also widespread, as presented in papers, such as the reviews by Ferraresi et al. [38] and Leal-Júnior [6]. Therefore, physics variables, such as power and total energy applied, and the distance between the points of the application by such

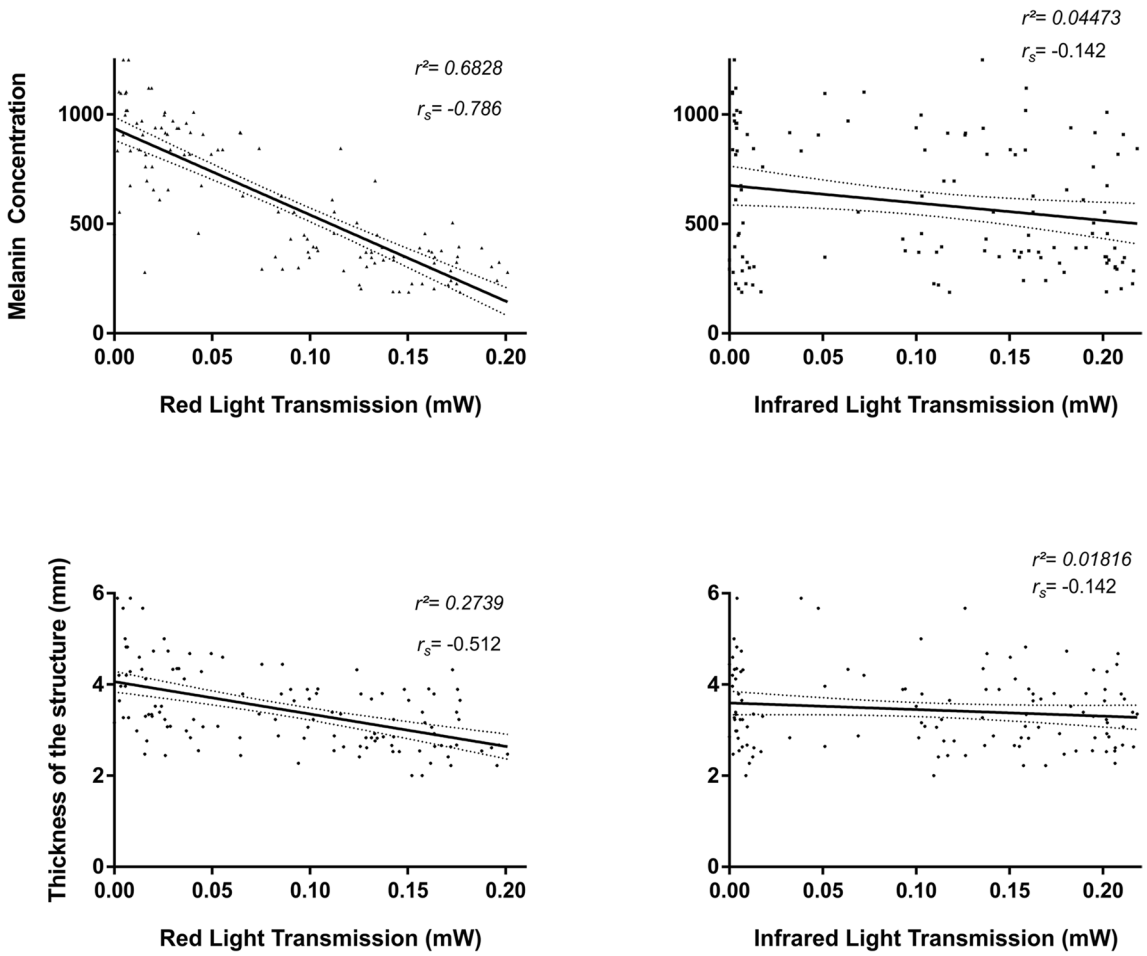


**Fig. 3** A linear regression with a 95% confidence bands and the correlation between transmitted power and different melanin index and thickness in the "skin-skin" condition

equipment should also be considered. Guirro and collaborators [37] highlighted a distance of 1 cm between the LEDs, thus making something close to the findings of our study of length for overlapping power transmitted. However, each device has different layouts, and this should be considered for the desired effect.

Considering the need to know the biophysical conditions of light for therapeutic interventions, Salehpour et al. [39] conducted a literature review on the penetration profiles of lasers and light-emitting diodes, both in the visible and near-infrared spectrum, but in human and animal skull tissues such as rabbits, rats, and mice. His group points out that while the power of the emitting source is an obvious determinant for penetration, individual characteristics are additional, less predictable variables, making it challenging to develop the application of transcranial photobiomodulation. Among these particular characteristics, there is clinical availability, evaluation, and Fitzpatrick's scale classically indicates the definition of phototype. Md Isa et al. [26] conducted a correlation study between the Mexameter values and the Fitzpatrick's scale. Their findings suggest that our volunteers would present matters, such as index II and III for the light skin group and V and VI for the dark skin group.

Compared with our results, the thicker structures present less transmissivity due to the light decay (absorption and scattering). However, individual conditions can alter the clinical outcome, among them the melanin index. Other characteristics of the light-generating source should be considered, such as the divergence of the beam, which may promote a decrease in power, i.e., when we measure the transmitted power, it is lower by two factors, attenuation (either by absorption or scattering), and by the divergence of the beam. Individual factors can be observed, as in the studies by Cruz-Júnior et al. [20, 21], indicating a high association between greater penetration capacity and a longer wavelength. Longer spectra appear to exhibit less interaction with the melanin chromophore. Furthermore, Ash et al. [14] demonstrated that in addition to biological individualities, factors such as beam diameter and lateral profile also influence transmission. These findings, therefore, align with the

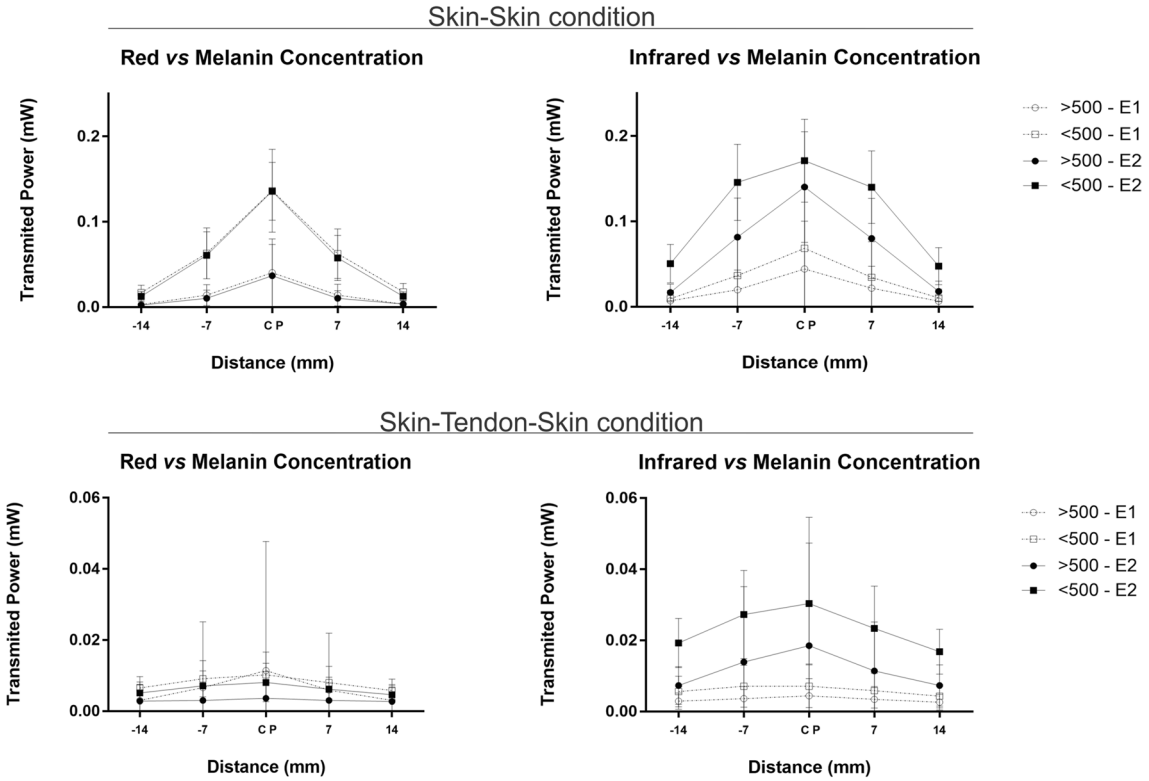


**Fig. 4** Distribution of transmitted power, considering the position of the laser emitter in the central point (CP), measured with five photodiodes positioned at −14, −7, CP, 7, and 14 mm. E1: equipment 1; E2: equipment 2; mW: milliwatts; CP: center point; <500 and >500: melanin index

existing literature. Additionally, given the sensitivity of the available sensors, they are suitable for acquisition and interaction, considering that the aim of this study is to observe and demonstrate the attenuation profile rather than focusing on absolute values.

Bordvik et al. [40] conducted a study to evaluate the transmission profiles of two human Achilles tendon lasers in situ, under resting and elongated conditions with two different therapeutic lasers, one of 904 nm with 60 mW of mean output power (MOP), and one of 810 nm with 200 mW of MOP. Their results indicate that the 904-nm laser penetrates more than the 810-nm laser in the target tissue. Such work is in line with our findings when we observe that longer wavelengths have greater transmission capacity, as already pointed out by the literature [41]. However, when we compared our results with those presented by Bordvik's group, the mean power found by them in the relaxed calcaneus tendon (same condition as the one applied by the present study) was expressively superior. Possibly, by not contemplating aspects, such as the divergence of the beam and its scattering, it may have generated greater values of power. Collecting the transmitted power at a single point with a sensor that presents a capture area more extensive than the irradiation area of the applicator does not consider the scattering and possible divergence of the beam. Thus, as the emission area of the applicator was smaller than the capture area, the use of a single sensor with an extensive area may have generated an overestimated result. Also, the population comprised of the two experimental designs, in which there are apparent differences in thickness and other individual characteristics, should be considered.

The "skin-tendon-skin" transmissivity values of our study indicate that the laser was not able to cross the tissues with significant power. The lack of greater value in the central point suggests that the sensors captured the diffused light, resulting from its reflection and refraction inside the skin and not its direct transmission in the tissues. This analysis was only possible by the disposition of the five sensors in the same line, with the irradiation and the simultaneous collection of the laser in the five sensors.

Another variable explored is the different beam diameters of the emitting sources. Such size has important clinical implications due to its effect on the transmissivity and scattering of light in the tissue. Ash et al. [14] pointed out that the increase in beam diameter presents a reduction in the amount of lateral scattering, apparently allowing greater penetration. Thus, our findings corroborate with such data; although an emitting source shows smaller values of applicator area, its divergence and consequent diameter of the

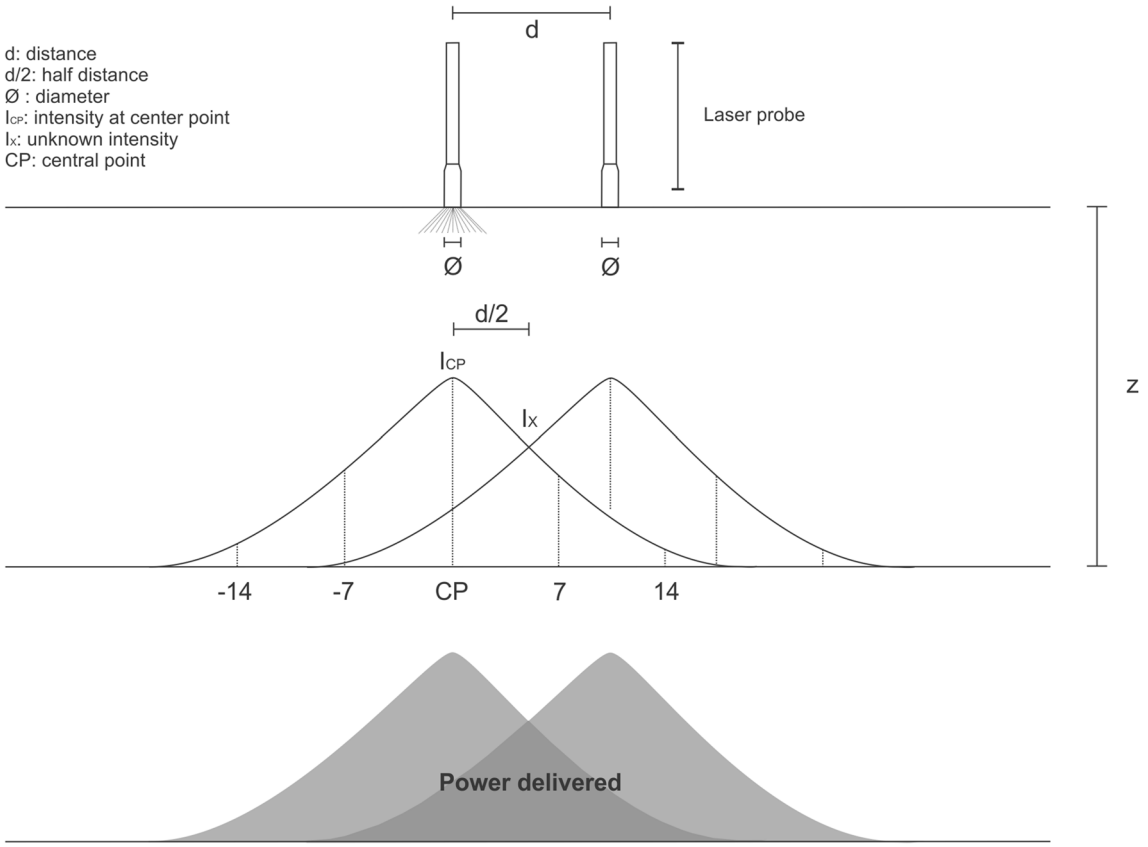


**Fig. 5** Distance between different points of application and its clinical implication

**Table 5** Distance between two points of application, considering 50% of the irradiated power

| Equipment | The distance of application between the points (mm) | |
|---|---|---|
| | > 500 | < 500 |
| E1–660 nm | 14.7 | 21.3 |
| E2–660 nm | 13.5 | 20.1 |
| E1–830 nm | 16.7 | 27.0 |
| E2–830 nm | 22.7 | 24.8 |

*E1* Equipment 1; *E2* equipment 2; <500 and >500: melanin index

effective light output show higher values of transmitted power when compared to another emitting source, with a smaller beam diameter (Table 1).

As a possibility to improve the transmissivity of laser in human skin tissue, Deng et al. [42] proposed using topical treatment of glycerol at different temperatures over the region to be irradiated. In their study, they used scanning lasers in the range of 400 to 1400 nm with a 10 nm interval, where data of 630 nm were obtained for quantitative analysis. They applied them in four different temperatures (4, 25, 32, and 45 °C). The two highest temperatures presented results, such as a decrease of dispersion in 61.6% and 76.6% and increased penetration depth in 53.3% and 84.1%, respectively. These results can alter the clinical outcome of an application, given the greater ease of penetration, considering that greater powers can reach the target tissues, including, consequently, a possibility of adjustments due to individual characteristics, as pointed out by Salehpour et al. [39].

In the same line, Haslerud et al. [43] applied 20 min of ice previously to laser irradiation (810 nm/200 mW and 904 nm/60 mW). They observed a significant increase in light penetration through the Achilles tendon in healthy individuals. These findings occurred in the presence of a significant reduction in skin temperature and Achilles tendon thickness. Hu et al. [44] reported that they could reach a depth of approximately 50 mm below the surface of structures comprising skin, bone, muscle, tendons, and ligaments, regardless of skin tone 660-nm laser. These findings are possibly due to methodological conditions in which scattering and reflection were discarded, indicating a low level of evidence.

Highlighting the optical effects of the skin, one should consider that the photons that penetrate the tissue can be

transmitted, scattered, or absorbed, and the scattering increases the volume of irradiated tissue since the photons can change direction without loss in energy density [41–45]. Thus, analyzing the lateral scattering between the application points, Ash et al. [14] suggest that a smaller beamwidth is associated with increased scattering and, as the beam width is increased, the photon spread becomes more and more projected forward to the critical point where the scattering in the saturated medium is. Thus, one can observe higher central values for the larger beam widths, as shown in Fig. 4. Our findings show that the transmissivity of red light depends on the amount of melanin, where a smaller amount enables a greater transmissivity. Yet, it seems to have no relation with the irradiance, having seen the different values presented between the two emitting sources analyzed here.

Otherwise, for the near-infrared light, the transmissivity depends on the amount of melanin in a smaller proportion, since in the group with a higher index (>500-E2), a higher transmissivity occurred than in the group with a lower index (<500-E1). These results send us the beam collimation parameters, indicating that the equipment with a larger beam diameter presents a greater transmission depth, reaching deeper tissues. This factor is even more important than the amount of melanin in near-infrared spectrum irradiation since, among the same equipment, melanin maintained the pattern of allowing a greater transmissivity when in a lower index.

In turn, considering the distance between the points of application, the literature presents a wide window, little of which is evaluated and discussed, shown in the light of our empirical knowledge. Our findings point out that for the application in the form of points, one should consider a distance between 16.7 and 27 mm for the near-infrared laser, considering light skin or dark skin. For red radiation, a smaller value should be considered so that at least 50% of the irradiated laser (13.5 to 21.3 mm) overlap also depends on the melanin index and the equipment used. Thus, we emphasize that not only the characteristics of the individuals will interfere with the laser scattering but also the generating source or, more specifically, the geometry of the beam and the wavelength.

For the "skin-tendon-skin" condition, whether in low or high melanin index, we understand that the capture of light occurred by scattering on the skin and not by transposing the tendon, making no sense to discuss the scattering for this situation. As shown in Fig. 4, the light is almost equally scattered by all the photodiodes, not making a central point of greater transmission and lateral decay. Still, as explored by Table 4, the values at 100% of the tissue transmission present too much power for discussion.

Finally, as pointed out by Jacques' study [46], a projection of the average distance between the application points can be pointed out in our findings. Thus, according to the Eq. (3):

$$\left(\frac{\lambda 1}{\lambda 2}\right)^{0.84} \times \text{average scattering} = \text{projected distance} \quad (3)$$

where λ1 is the wavelength with unknown scattering, λ2 is the wavelength with known scattering, 0.84 is the $\lambda^{-b}$ dependence, and average scattering is related to the known value for λ2. The average scattering can be interpreted as one that can effectively comprise an area with a power that reaches therapeutic values, even if it requires a second application, as presented here.

Thus, for example, in our study, this can be expressed as:

$$\left(\frac{830}{660}\right)^{0.84} \times 14.7 = 17.8 \text{ mm}$$

For this, we considered 660 nm like a known wavelength, 830 nm like an unknown scattering of wavelength, and 14.7 mm is the average scattering shown by our study. So, a scattering of 17.8 mm was reached close to that demonstrated by our applied methods. For example, another wavelength usually used in studies and clinical practice is 904 nm. Applying equation 3, we have reached an average scattering close to 19.1 mm. Thus, our study can be used as a form to extrapolated average scattering in different scenarios, as long as it is considered to be only a mathematical projection. This tool can be useful to give predictions for different wavelengths and thus facilitate the application of different equipment and different conditions. At present, to our knowledge, this is not well established. Additionally, it should be noted that this tool is useful not only for rehabilitation but also in the area of diagnostics. Tools such as OCT are a non-invasive technology used to obtain high-resolution images with different penetration depths, potentially providing the necessary diagnosis [47]. Since diagnosis is made by light-tissue interaction, the data presented here can assist in the first interaction between light and skin.

Our study presents limitations, such as the non-evaluation of humidity and skin elasticity, where other studies, as discussed here, point to a factor that interferes with the passage of light, thus diminishing replication in different age groups. Therefore, our results show itself with low extrapolation to other age groups. Still, it should be noted that the power obtained was evaluated after the transposition of two layers of skin, and the value of 50%

of thickness is a mathematical extrapolation. For this reason, further studies are necessary, inserting different skin tones and different ages, hydration conditions, and exploring different wavelengths. It is also interesting to analyze ex-vivo samples, with the interaction after one skin layer, given the possible difference between biological data and the mathematical extrapolation employed here.

## Conclusion

Laser transmission and scattering in vivo tissues are related to wavelength, beam diameter, thickness, and target tissue type, as well as melanin index. The 830-nm laser presents higher transmission on the skin when compared to 660 nm. It is suggested the distances between 13.5 and 27.0 mm between the application points, considering the red and near-infrared spectra, melanin index, and characteristics of the light-emitting source should have a uniform irradiated power. For the "skin-tendon-skin" irradiation, no significant penetration of the 660 and 830 nm lasers in the tissues was observed. Further studies are needed to describe the interaction of different skin tones, ages, hydration conditions and explore different wavelengths. Additionally, it should be noted that different equipment can generate significant differences in transmitted power as different physical conditions are imposed.

**Author contribution** All authors contributed to the study's conception and design. Material preparation and data collection were performed by Carlos Eduardo Girasol, José Miguel Andrade Ferraz Moraes, and Damião Miranda Ngonga Alfredo. The analysis was performed by Carlos Eduardo Girasol and Luciano Bachmann. The first draft of the manuscript was written by Carlos Eduardo Girasol, and all authors commented on previous versions of the manuscript. All authors read and approved the final manuscript.

**Funding** The present work was supported in part by The Sao Paulo Research Foundation – FAPESP (#2018/14955-6, #2017/25923-5, and 2011/07960-4), in part by the Coordination for the Improvement of Higher Education Personnel - Brazil (CAPES) – Financing Code 001, and in part by Scholarship from National Institute for Scholarship Management (INAGBE), Angola.

**Data availability** It can be made available upon request.

**Code availability** Not applicable.

## Declarations

**Ethics approval** This study was approved by the Ethics Committee of the Clinics Hospital of the Medical School of Ribeirão Preto, under protocol 2.748.430.

**Consent to participate** The volunteers were informed about the research project, its objectives, and its characteristics, and all signed the consent form.

**Consent for publication** The volunteers and authors consent to publish this data and work.

**Competing interests** The authors declare no competing interests.

## References

1. Anders JJ, Arany PR, Baxter GD, Lanzafame RJ (2019) Light-emitting diode therapy and low-level light therapy are photobiomodulation therapy. Photobiomodul Photomed Laser Surg 37:63–65. https://doi.org/10.1089/photob.2018.4600
2. Cheng K, Martin LF, Slepian MJ et al (2021) Mechanisms and pathways of pain photobiomodulation: a narrative review. J Pain 22:763–777. https://doi.org/10.1016/j.jpain.2021.02.005
3. Kashiwagi S, Morita A, Yokomizo S et al (2023) Photobiomodulation and nitric oxide signaling. Nitric Oxide 130:58–68. https://doi.org/10.1016/j.niox.2022.11.005
4. Karu TI (2010) Multiple roles of cytochrome c oxidase in mammalian cells under action of red and IR-A radiation. IUBMB Life 62:607–610. https://doi.org/10.1002/iub.359
5. Nampo FK, Cavalheri V, dos Santos SF et al (2016) Low-level phototherapy to improve exercise capacity and muscle performance: a systematic review and meta-analysis. Lasers Med Sci 31:1957–1970. https://doi.org/10.1007/s10103-016-1977-9
6. Leal-Junior ECP, Vanin AA, Miranda EF et al (2015) Effect of phototherapy (low-level laser therapy and light-emitting diode therapy) on exercise performance and markers of exercise recovery: a systematic review with meta-analysis. Lasers Med Sci 30:925–939. https://doi.org/10.1007/s10103-013-1465-4
7. das Neves LMS, de Leite G PMF, Marcolino AM et al (2017) Laser photobiomodulation (830 and 660 nm) in mast cells, VEGF, FGF, and CD34 of the musculocutaneous flap in rats submitted to nicotine. Lasers Med Sci 32:335–341. https://doi.org/10.1007/s10103-016-2118-1
8. de Souza TR, de Souza AK, Garcia SB et al (2020) Photobiomodulation increases viability in full-thickness grafts in rats submitted to nicotine. Lasers Surg Med 52:449–455. https://doi.org/10.1002/lsm.23155
9. Kingsley JD, Demchak T, Mathis R (2014) Low-level laser therapy as a treatment for chronic pain. Front Physiol 5. https://doi.org/10.3389/fphys.2014.00306
10. Oueslati A, Lovisa B, Perrin J et al (2015) Photobiomodulation suppresses alpha-synuclein-induced toxicity in an AAV-based rat genetic model of Parkinson's disease. PLoS One 10:e0140880. https://doi.org/10.1371/journal.pone.0140880
11. Hamblin MR (2018) Mechanisms and mitochondrial redox signaling in photobiomodulation. Photochem Photobiol 94:199–212. https://doi.org/10.1111/php.12864
12. Bjordal JM (2012) Low level laser therapy (LLLT) and world association for laser therapy (WALT) dosage recommendations. Photomed Laser Surg 30:61–62. https://doi.org/10.1089/pho.2012.9893
13. Anderson RR, Parrish JA (1981) The optics of human skin. J Investig Dermatol 77:13–19. https://doi.org/10.1111/1523-1747.ep12479191
14. Ash C, Dubec M, Donne K, Bashford T (2017) Effect of wavelength and beam width on penetration in light-tissue interaction

using computational methods. Lasers Med Sci 32:1909–1918. https://doi.org/10.1007/s10103-017-2317-4
15. Barbosa RI, Guirro ECO, Bachmann L et al (2020) Analysis of low-level laser transmission at wavelengths 660, 830 and 904 nm in biological tissue samples. J Photochem Photobiol B 209:111914. https://doi.org/10.1016/j.jphotobiol.2020.111914
16. Fallah A, Mirzaei A, Gutknecht N, Demneh AS (2017) Clinical effectiveness of low-level laser treatment on peripheral somatosensory neuropathy. Lasers Med Sci 32:721–728. https://doi.org/10.1007/s10103-016-2137-y
17. Ökmen BM, Ökmen K (2017) Comparison of photobiomodulation therapy and suprascapular nerve-pulsed radiofrequency in chronic shoulder pain: a randomized controlled, single-blind, clinical trial. Lasers Med Sci 32:1719–1726. https://doi.org/10.1007/s10103-017-2237-3
18. Sasso LL, de Souza LG, Girasol CE et al (2020) Photobiomodulation in sciatic nerve crush injuries in rodents: a systematic review of the literature and perspectives for clinical treatment. J Lasers Med Sci 11:332–344. https://doi.org/10.34172/jlms.2020.54
19. Nussbaum EL, Van Zuylen J, Jing F (2007) Transmission of light through human skin folds during phototherapy: effects of physical characteristics, irradiation wavelength, and skin-diode coupling. Physiotherapy Canada 59:194–207. https://doi.org/10.3138/ptc.59.3.194
20. da Cruz LB, Girasol CE, Coltro PS et al (2023) Optical properties of human skin phototypes and their correlation with individual angle typology. Photobiomodul Photomed Laser Surg 41:175–181. https://doi.org/10.1089/photob.2022.0111
21. Cruz Junior LB, Girasol CE, Coltro PS et al (2023) Absorption and reduced scattering coefficient estimation in pigmented human skin tissue by experimental colorimetric fitting. J Opt Soc Am A 40:1680. https://doi.org/10.1364/JOSAA.489892
22. Cheong WF, Prahl SA, Welch AJ (1990) A review of the optical properties of biological tissues. IEEE J Quantum Electron 26:2166–2185. https://doi.org/10.1109/3.64354
23. Jacques SL (2013) Optical properties of biological tissues: a review. Phys Med Biol 58:R37–R61. https://doi.org/10.1088/0031-9155/58/11/R37
24. Bashkatov AN, Genina EA, Tuchin VV (2011) Optical properties of skin, subcutaneous, and muscle tissues: a review. J Innov Opt Health Sci 04:9–38. https://doi.org/10.1142/S1793545811001319
25. Bogdan Allemann I, Kaufman J (2011) Laser principles. Curr Probl Dermatol 42:7–23. https://doi.org/10.1159/000328236
26. Md Isa Z, Shamsuddin K, Bukhary Ismail Bukhari N et al (2016) The reliability of Fitzpatrick Skin Type Chart Comparing to Mexameter (Mx 18) in measuring skin color among first trimester pregnant mothers in Petaling District, Malaysia. Malaysian J Public Health Med 16:59–65
27. Niemz MH (2019) Matter acting on light. In: laser-tissue interactions. Springer International Publishing, Cham, pp 9–44
28. Mendenhall MJ, Nunez AS, Martin RK (2015) Human skin detection in the visible and near infrared. Appl Opt 54:10559. https://doi.org/10.1364/AO.54.010559
29. Berger VW, Zhou Y (2014) Kolmogorov–Smirnov test: overview. In: Wiley StatsRef: Statistics Reference Online. Wiley
30. McKight PE, Najab J (2010) Kruskal-Wallis test. In: The Corsini Encyclopedia of Psychology. Wiley, pp 1–1
31. Myers L, Sirois MJ (2006) Spearman correlation coefficients, differences between. In: Encyclopedia of Statistical Sciences. John Wiley & Sons, Inc, Hoboken, NJ, USA
32. Kolárová H, Ditrichová D, Wagner J (1999) Penetration of the laser light into the skin in vitro. Lasers Surg Med 24:231–235
33. Enwemeka CS (2000) Attenuation and penetration of visible 632.8nm and invisible infra-red 904nm light in soft tissues. Laser Ther 13:95–101. https://doi.org/10.5978/islsm.13.95
34. Joensen J, Øvsthus K, Reed RK et al (2012) Skin penetration time-profiles for continuous 810 nm and superpulsed 904 nm lasers in a rat model. Photomed Laser Surg 30:688–694. https://doi.org/10.1089/pho.2012.3306
35. Anders JJ, Wu X (2016) Comparison of light penetration of continuous wave 810 nm and superpulsed 904 nm wavelength light in anesthetized rats. Photomed Laser Surg 34:418–424. https://doi.org/10.1089/pho.2016.4137
36. de Jesus Guirro RR, de Oliveira Guirro EC, Martins CC, Nunes FR (2010) Analysis of low-level laser radiation transmission in occlusive dressings. Photomed Laser Surg 28:459–463. https://doi.org/10.1089/pho.2009.2524
37. de Jesus Guirro RR, de Carvalho G, Gobbi A et al (2020) Measurement of physical parameters and development of a light emitting diodes device for therapeutic use. J Med Syst 44:88. https://doi.org/10.1007/s10916-020-01557-y
38. Ferraresi C, Huang Y-Y, Hamblin MR (2016) Photobiomodulation in human muscle tissue: an advantage in sports performance? J Biophotonics 9:1273–1299. https://doi.org/10.1002/jbio.201600176
39. Salehpour F, Cassano P, Rouhi N et al (2019) Penetration profiles of visible and near-infrared lasers and light-emitting diode light through the head tissues in animal and human species: a review of literature. Photobiomodul Photomed Laser Surg 37:581–595. https://doi.org/10.1089/photob.2019.4676
40. Bordvik DH, Haslerud S, Naterstad IF et al (2017) Penetration time profiles for two class 3B lasers in *in situ* human Achilles at rest and stretched. Photomed Laser Surg 35:546–554. https://doi.org/10.1089/pho.2016.4257
41. Enwemeka CS (2009) Intricacies of dose in laser phototherapy for tissue repair and pain relief. Photomed Laser Surg 27:387–393. https://doi.org/10.1089/pho.2009.2503
42. Deng Z, Liu C, Tao W, Zhu D (2011) Improvement of skin optical clearing efficacy by topical treatment of glycerol at different temperatures. J Phys Conf Ser 277:012007. https://doi.org/10.1088/1742-6596/277/1/012007
43. Haslerud S, Naterstad IF, Bjordal JM et al (2017) Achilles tendon penetration for continuous 810 nm and superpulsed 904 nm lasers before and after ice application: an in situ study on healthy young adults. Photomed Laser Surg 35:567–575. https://doi.org/10.1089/pho.2017.4269
44. Hu D, van Zeyl M, Valter K, Potas JR (2019) Sex, but not skin tone affects penetration of red-light (660 nm) through sites susceptible to sports injury in lean live and cadaveric tissues. J Biophotonics 12. https://doi.org/10.1002/jbio.201900010
45. Henderson TA, Morries L (2015) Near-infrared photonic energy penetration: can infrared phototherapy effectively reach the human brain? Neuropsychiatr Dis Treat 2191. https://doi.org/10.2147/NDT.S78182
46. Jacques SL (2010) Optical assessment of cutaneous blood volume depends on the vessel size distribution: a computer simulation study. J Biophotonics 3:75–81. https://doi.org/10.1002/jbio.200900085
47. Turani Z, Fatemizadeh E, Blumetti T et al (2019) Optical radiomic signatures derived from optical coherence tomography images improve identification of melanoma. Cancer Res 79:2021–2030. https://doi.org/10.1158/0008-5472.CAN-18-2791